IOPscience iopscience.iop.org

Home Search Collections Journals About Contact us My IOPscience

The magnetic structures of $YbMn_2Si_2$

This article has been downloaded from IOPscience. Please scroll down to see the full text article.

2001 J. Phys.: Condens. Matter 13 9773

(http://iopscience.iop.org/0953-8984/13/43/308)

View the table of contents for this issue, or go to the journal homepage for more

Download details:
IP Address: 171.66.16.226
The article was downloaded on 16/05/2010 at 15:03

Please note that terms and conditions apply.

INSTITUTE OF PHYSICS PUBLISHING JOURNAL OF PHYSICS: CONDENSED MATTER

J. Phys.: Condens. Matter **13** (2001) 9773–9780 PII: S0953-8984(01)26242-0

The magnetic structures of $YbMn_2Si_2$

M Hofmann[1,2], S J Campbell[3], A V J Edge[3] and A J Studer[4]

[1] Rutherford Appleton Laboratory, ISIS, Chilton, DIDCOT, OX11 0QX, UK
[2] Hahn-Meitner-Institut, BENSC, Berlin, Germany
[3] School of Physics, University College, The University of New South Wales, Australian Defence Force Academy, Canberra, ACT 2600, Australia
[4] Neutron Scattering Group, ANSTO, Lucas Heights Research Laboratories, Menai, NSW 2234, Australia

E-mail: M.Hofmann@rl.ac.uk

Received 27 June 2001, in final form 31 August 2001
Published 12 October 2001
Online at stacks.iop.org/JPhysCM/13/9773

Abstract

The magnetic structures of $YbMn_2Si_2$ with the tetragonal $ThCr_2Si_2$-type structure have been determined by neutron diffraction measurements over the temperature range ∼1.5–538 K. Rietveld refinements demonstrate that $YbMn_2Si_2$ has a collinear antiferromagnetic structure below the Néel temperature $T_{N1} = 526(4)$ K with the Mn moments parallel to the c-axis. Below $T_{N2} \sim 30(5)$ K, the Mn sublattice rearranges to a +−−+ antiferromagnetic structure with propagation vector $\boldsymbol{k} = 00\frac{1}{2}$. The moment direction is along the c-axis with a total moment of 1.92(8) μ_B at 10 K. There is no indication of ordering of the Yb ions at 10 K, although a diffraction pattern at 1.5 K shows that the Yb ions are ordered at the latter temperature. Analysis reveals that the Yb sublattice orders antiferromagnetically. The antiferromagnetically ordered Yb sublattice exhibits the same propagation vector, $\boldsymbol{k} = 00\frac{1}{2}$, as the Mn sublattice, although the Yb spin directions are found to be perpendicular to the c-axis compared with the parallel alignment of the Mn moments. The refined value of the Yb^{3+} magnetic moment at 1.5 K is $\mu_{Yb} = 0.57(9)\ \mu_B$ compared with the free ion value of about 4.5 μ_B, while at 1.5 K the Mn magnetic moment is $\mu_{Mn} = 1.98(7)\ \mu_B$.

1. Introduction

Rare earth ions in intermetallic compounds with the formula RT_2X_2 (R = rare earth, T = transition metal and X = Si, Ge) are generally in a 3+ valence state. However, because of the greater stability of the empty, half-filled or filled 4f shells, the Ce, Sm, Eu, Tm and Yb ions may also exist in other valence states, resulting in compounds that exhibit unusual physical and magnetic properties. As an example, Eu is divalent in $EuMn_2Ge_2$ and orders magnetically at low temperatures whereas $EuMn_2Si_2$ exhibits a fluctuating valence state, thus leading to a valence transition in $EuMn_2Si_{2-x}Ge_x$ around the Ge concentration $x \sim 0.075$ [1]. Other

 © 2001 IOP Publishing Ltd Printed in the UK

examples of unusual behaviour include (i) an increase in the effective value of the Yb valence in $YbNi_2(Ge_{1-x}Si_x)_2$ on compression of the lattice by substitution of Ge for Si and formation of a region ($x = 0.1$–0.9) in which the Yb ions are in the Kondo state [2] and (ii) the unusual lattice expansion (attributed to valence state fluctuations) exhibited by $YbMn_2Ge_2$ [3].

While the overall magnetic behaviour of $YbMn_2Si_2$ has been investigated previously by magnetic and Mössbauer effect spectroscopic measurements [4, 5], the magnetic structure of $YbMn_2Si_2$ has so far not been determined. We have therefore carried out a neutron powder diffraction investigation of $YbMn_2Si_2$ over the temperature range ∼1.5–538 K. Three distinct magnetic regions have been found for $YbMn_2Si_2$: first, a collinear antiferromagnetic region which exists below the Néel temperature $T_{N1} = 526(4)$ K. This antiferromagnetic order then gives way to an unusual +−−+ antiferromagnetic rearrangement of the Mn magnetic sublattice below $T_{N2} \sim 30$ K, with the third region indicating ordering of the Yb^{3+} ions at 1.5 K, the lowest temperature attained.

2. Experimental details

The sample was prepared from high-purity elements (Yb 99.9%, Mn 99.99% and Si 99.999%) using an arc furnace with an argon pressure of about 1 bar. The starting materials contained ∼10% excess Yb and ∼2% excess Mn to compensate for evaporation losses during melting. X-ray and neutron powder diffraction measurements reveal the predominant reflections of the tetragonal 1:2:2 structure as expected, although ∼1.5(1.0)% of the Yb_2O_3 phase is also found to be present (see figure 1). A very small fraction of another impurity phase, probably YbMnSi, can also be discerned in the diffraction patterns, but due to its small content, $< \sim 1\%$, the phase was not included in the refinements.

An initial set of neutron powder diffraction patterns was obtained using the MRPD diffractometer, Reactor HIFAR and Lucas Heights over the temperature range ∼10–300 K. Further, a more comprehensive set of neutron diffraction patterns (focussing on the temperature regions over which changes in the magnetic behaviour were discerned) was obtained over the temperature range ∼1.5–538 K on the E6 diffractometer at the Hahn-Meitner-Institut, Berlin (wavelength $\lambda = 2.448$ Å). In both cases, the variable temperature measurements were carried out with the sample placed in a vanadium can and mounted in a standard cryostat. A good agreement was obtained over common temperature regions between both sets of data. The Rietveld refinements were carried out on the E6 data using the Fullprof [6] program package which allows simultaneous refinement of the structural and magnetic parameters. Using the coherent scattering lengths for all the elements and the magnetic form factor for Mn as given in [7], the parameters that varied during the initial least-square refinements included a scale factor for each phase, two parameters for the background, the lattice constants and a positional parameter for the Si atoms in the $YbMn_2Si_2$ compound. Finally, the Mn and Yb magnetic moment values as well as an overall temperature factor were refined.

3. Results and discussion

Figure 1 shows four of the neutron powder diffraction patterns obtained over the temperature range ∼1.5–538 K. As expected, the pattern at ∼538 K (figure 1(a)) reveals reflections which are characteristic of the tetragonal body centred $ThCr_2Si_2$-type structure ($I4/mmm$). As noted above, the sample contained ∼1.5(1.0)% of the Yb_2O_3 phase which is also included in the refinements.

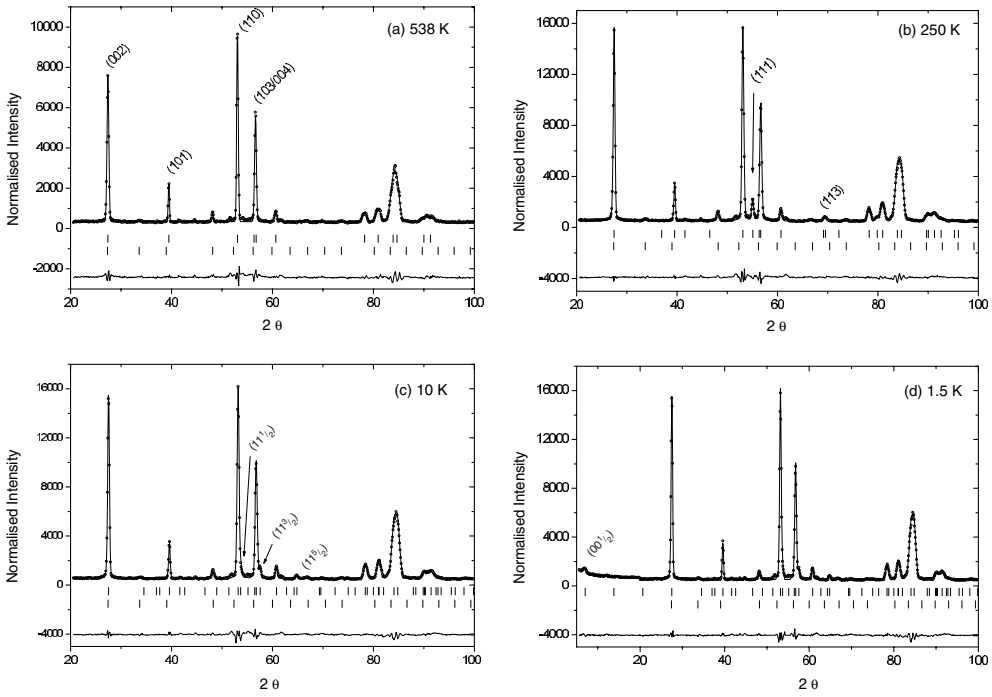

Figure 1. Rietveld refinements to the neutron diffraction patterns of the $YbMn_2Si_2$ sample at the temperatures indicated. Several (*hkl*) reflections are marked for each pattern as discussed in the text. The markers for $YbMn_2Si_2$ (top) and the major impurity Yb_2O_3 phase (∼1.5%, bottom) are also shown.

The different magnetic features of $YbMn_2Si_2$ are indicated by the 250, 10 and 1.5 K diffraction patterns of figure 1. The 250 K diffraction pattern (figure 1(b)) reveals additional intensity in the (111), (113) and (201) peaks. These reflections are of the type $h + k + l = 2n + 1$ and lead to refinement of the 250 K pattern based on a collinear antiferromagnetic structure. This structure (ferromagnetic Mn (00*l*) planes coupled antiferromagnetically along the *c*-axis, figure 2(a)) is common to many of the RMn_2Si_2 series (e.g. YMn_2Si_2 [8]) and can be labelled as AF*il* using the notation of Venturini *et al* [9]. The variation of the (111) peak intensity with temperature (figure 3) leads to an antiferromagnetic ordering temperature of $T_{N1} \sim 526(4)$ K, which is in good agreement with the values of ∼513 K [4] and ∼520 K [5] determined from previous magnetic measurements. ($T_{N1} \sim 526(4)$ K was determined from the function given in the caption to figure 3; this expression provides a convenient empirical function to represent the trends of the data.) This behaviour is expected for $YbMn_2Si_2$ as at all temperatures below the transition temperature $T_{N1} \sim 526$ K, the value of the in-plane Mn–Mn spacings, $d_{Mn–Mn} <$ ∼2.85 Å (e.g. $d_{Mn–Mn} \sim 2.760$ Å and ∼2.744 Å for $YbMn_2Si_2$ at ∼520 K and ∼10 K, respectively). This value of $d_{Mn–Mn}$ is the value below which antiferromagnetic coupling occurs between ferromagnetic (001) layers in these 1-2-2 compounds [10] (see also [9, 11]). It is concluded that the Mn sublattice of $YbMn_2Si_2$ exhibits the antiferromagnetic AF*il* structure shown in figure 2(a) below $T_{N1} \sim 526$ K to the temperature $T_{N2} \sim 30(5)$ K at which, as described below, we identify a rearrangement of the antiferromagnetic ordering scheme in the Mn sublattice. The structural and magnetic parameters of $YbMn_2Si_2$ as determined from the refinements to the diffraction patterns of figure 1 are given in table 1.

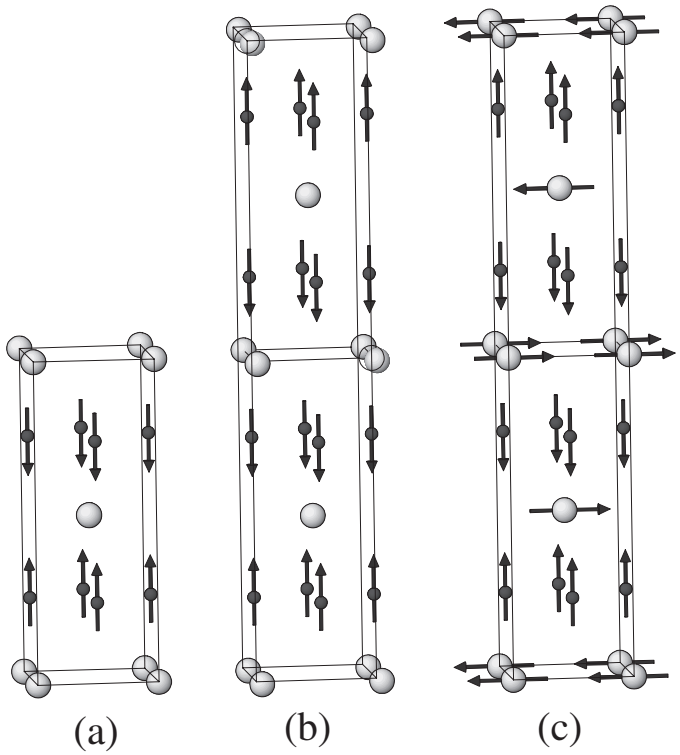

Figure 2. The antiferromagnetic structures of $YbMn_2Si_2$ (the Mn atoms are shown as small circles, and for clarity the Si atoms are not drawn): (a) $T = 250$ K; antiferromagnetic AF*il* structure of the Mn sublattice ($T_{N2} \sim 30$ K $< T < T_{N1} \sim 526$ K); (b) $T = 10$ K; antiferromagnetic $+--+$ structure of the Mn sublattice with propagation vector $\boldsymbol{k} = 001/2$ ($T < T_{N2} \sim 30$ K); (c) $T =$ 1.5 K; antiferromagnetic $+--+$ structures of the Mn and Yb sublattices; both exhibit the propagation vector, $\boldsymbol{k} = 00^{1}/_{2}$ $\left(T < T_N^{Yb}\right)$.

Table 1. Structural and magnetic data for $YbMn_2Si_2$ as determined from Rietveld refinements to neutron diffraction patterns at the temperatures indicated (cf. figure 1).

	$T = 1.5$ K	$T = 10$ K	$T = 250$ K	$T = 538$ K
a (Å)	3.8805(6)	3.8807(6)	3.8864(6)	3.9031(7)
c (Å)	10.382(2)	10.382(2)	10.404(2)	10.446(2)
z (Si)	0.3850(9)	0.3844(9)	0.3838(9)	0.387(2)
μ(Mn) [μ_B]	1.98(7)	1.92(8)	2.0(1)	–
μ (Yb) [μ_B]	0.57(9)	–	–	–

As the sample is cooled below ∼35 K, two interesting effects are observed: the intensities of the (111) and related reflections decrease and, commensurate with these decreases, additional reflections appear. These effects are indicated in detail in figure 4, which shows a region of the $YbMn_2Si_2$ diffraction patterns over the temperature range ∼1.5–45 K. As indicated by the temperature variation of the (111) peak intensity (inset to figure 4), the intensities of reflections of the type $h + k + l = 2n + 1$ decrease sharply at ∼30 K. This temperature marks the onset of a rearrangement of the magnetic ordering scheme. A

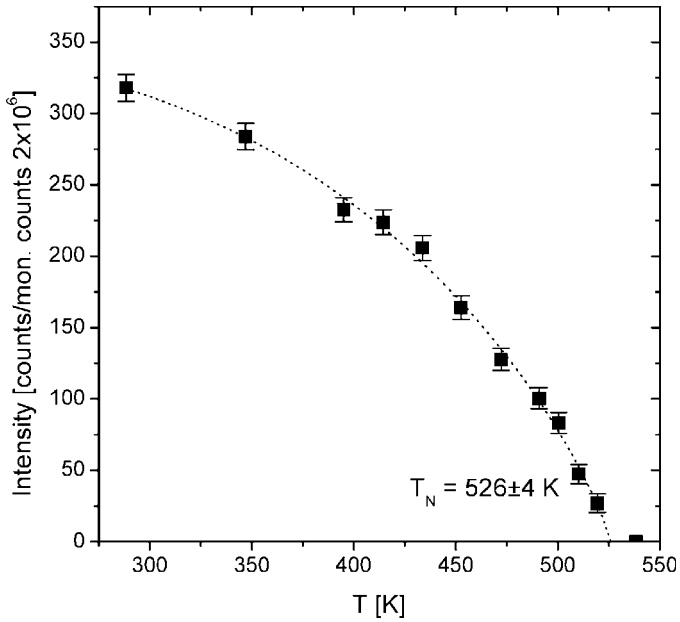

Figure 3. The variation of the intensity of the (111) reflection of $YbMn_2Si_2$ with temperature. The dashed line (based on a fit to the data) acts as a guide to the eye. The data were fitted to the expression $I(T) = c^*[1 - (T/T_N)^d]^e$ [12] leading to $T_N = 526(4)$ K, $d = 3.4(9)$ and $e = 0.8(1)$.

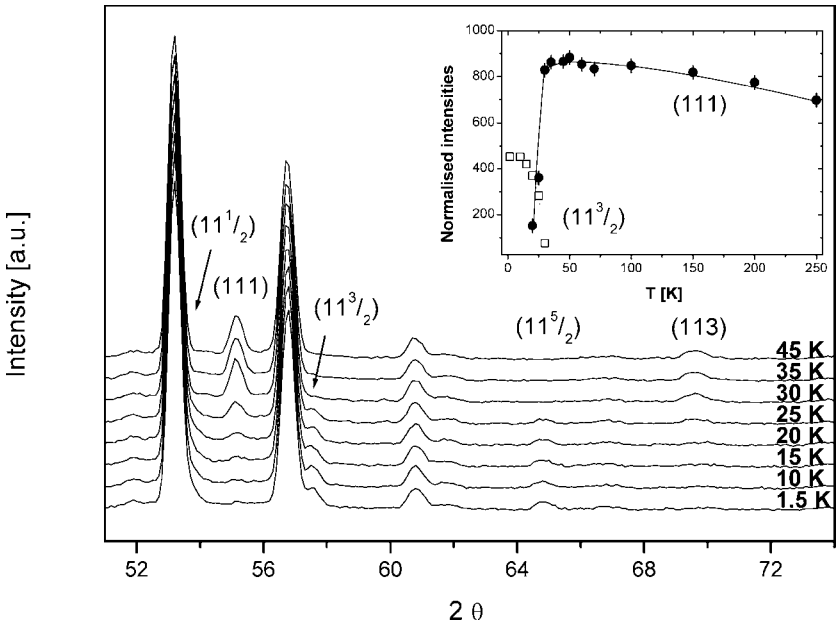

Figure 4. Part of the neutron diffraction patterns obtained for the $YbMn_2Si_2$ sample over the temperature range ∼1.5–45 K. The inset shows the variation of the intensity of the antiferromagnetic (111) reflection over the temperature range ∼1.5–250 K and the evolution of the $(11\frac{3}{2})$ reflection below $T_{N2} \sim 30(5)$ K.

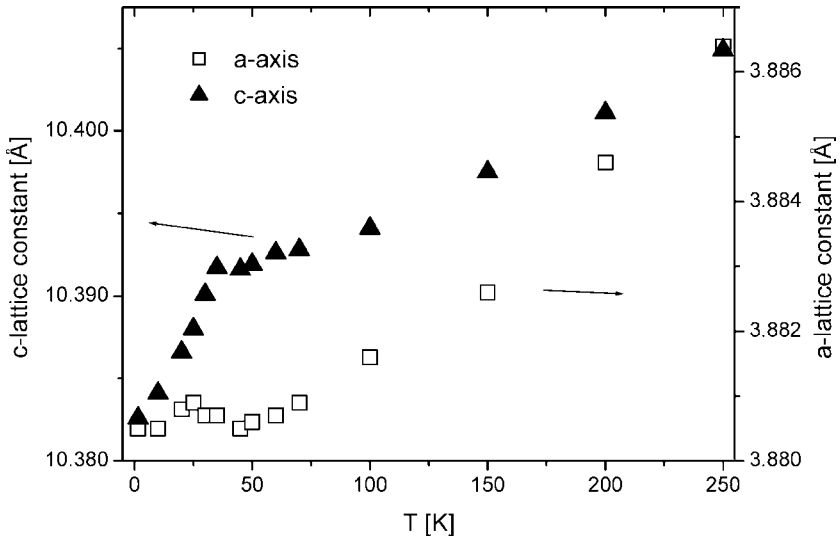

Figure 5. The variation of the a and c lattice parameters of $YbMn_2Si_2$ with temperature (∼1.5–300 K).

new set of magnetic peaks is found to occur below ∼30 K. Their intensities increase with decreasing temperature, and the peaks persists to ∼1.5 K, the lowest temperature attained in our experiments. These new magnetic peaks can be indexed by doubling the magnetic unit cell along the c-axis and, using the formalism of a magnetic propagation vector $\boldsymbol{k} = 00{}^1/_2$, can be indexed as $hkl \pm {}^1/_2$ (with $h + k = 2n$). The temperature dependence of the intensities of these new reflections is characterized by the behaviour of the $(11{}^1/_2)$ reflection (inset to figure 4). Given the absence of peaks with the reflection conditions $00l \pm {}^1/_2$ below ∼30 K, the Mn moments remain aligned along the c-axis in this temperature region. It should be noted that there is no evidence for the onset of Yb ordering at ∼30 K (particularly the absence of a reflection obeying the conditions $hkl \pm {}^1/_2$ with $h + k = 2n + 1$). Taking these features into account, the neutron pattern at 10 K (figure 1(c)) was refined using a model in which the Mn magnetic moments are arranged in a +−−+ sequence along the c-axis (figure 2(b)). Based on this model, the refinement to the 10 K pattern of figure 1(c) yields a magnetic moment of $\mu_{Mn} = 1.92(8)\ \mu_B$ (table 1). It is concluded that below a second Néel temperature $T_{N2} \sim 30(5)$ K, the Mn magnetic sublattice orders in the manner as shown in figure 2(b). The Mn moment value $\mu_{Mn} = 1.92(8)\ \mu_B$ at 10 K is slightly lower than the moment value $\mu_{Mn} = 2.1(1)\ \mu_B$ found in the AF*il* phase at $T = 45$ K. Antiferromagnetic ordering of the type +−−+ has been shown to occur commonly in the rare-earth sublattice in RT_2X_2 compounds (X = metalloid) such as $PrFe_2Si_2$ and $PrFe_2Ge_2$ [10] and $TmMn_2Ge_2$ [13]. However, to our knowledge this represents the first time that +−−+ antiferromagnetic ordering has been observed for the Mn sublattice in RT_2X_2 compounds.

Additional evidence in support of this second antiferromagnetic transition at $T_{N2} \sim 30(5)$ K is given by the variation of the a and c lattice parameters of $YbMn_2Si_2$ as shown in figure 5. Here, the c parameter exhibits a distinct change in its temperature dependence around ∼35 K with a pronounced decrease in c-values with decreasing temperature ($\Delta c/\Delta T \sim 270 \times 10^{-6}$ Å K^{-1} below T_{N2}, compared with the value $\Delta c/\Delta T \sim 65 \times 10^{-6}$ Å K^{-1} above T_{N2}). This deviation is likely to be linked with the reordering process along the c-axis with the doubling of the unit cell length associated with the $00{}^1/_2$ propagation vector. Values of the a lattice

parameter also exhibits a distinct but less pronounced change in their temperature dependence around T_{N2} (figure 5). The relatively gradual change in $\Delta c/\Delta T$ around ∼35 K indicates that the transition at T_{N2} is likely to be of the second order. This is also consistent with earlier magnetization measurements that revealed a peak in the susceptibility of $YbMn_2Si_2$ around 35 K [5], although further measurements (e.g. detailed magnetization, specific heat and ^{170}Yb Mössbauer spectroscopy) are required to confirm this suggestion. It should be noted that the magnetic transition observed by Nowik *et al* [5] around ∼35 K was linked with ordering of the trivalent Yb sublattice rather than the +−−+ antiferromagnetic ordering of the Mn sublattice as reported here.

A further new magnetic feature of $YbMn_2Si_2$ is revealed at $T = 1.5$ K (figure 1(d)); here we find a small additional peak at $2\theta \sim 6.8^\circ$ which can be indexed as a $(00\frac{1}{2})$ reflection on the basis of the propagation vector $\boldsymbol{k} = 00\frac{1}{2}$. As noted above, given that the magnetic reflections which obey the condition $hkl \pm \frac{1}{2}$ $(h + k = 2n)$ persist from $T_{N2} \sim 30$ K down to ∼1.5 K, the Mn sublattice remains antiferromagnetically ordered along the *c*-axis. It is noted that the appearance of the $(00\frac{1}{2})$ reflection could also be attributed to a tilting of the Mn moments away from the *c*-axis (see, e.g., $TmMn_2Ge_2$ [13]). However, there is an evidence for additional small magnetic features at $2\theta = 37.4^\circ$ and 42.3° in the neutron diffraction pattern of $YbMn_2Si_2$ at 1.5 K which can be indexed as $10\frac{1}{2}$ and $10\frac{3}{2}$ reflections, respectively. Given that these latter reflections cannot be generated by tilting of the Mn moments, it is concluded that this new $(00\frac{1}{2})$ reflection is due to the ordering of the Yb sublattice. The best refinements lead to a model in which the Yb moments are coupled antiferromagnetically +−−+ along the *c*-axis (while fitting in to the +−−+ ordering scheme of the Mn moments below T_{N2}) with the Yb moment direction perpendicular to the *c*-axis. The antiferromagnetic structure of $YbMn_2Si_2$ below T_N^{Yb}, the ordering temperature of the Yb sublattice, is shown in figure 2c (~ 1.5 K $< T_N^{Yb} <$ ∼10 K; note that no patterns were measured between ∼1.5 K and ∼10 K in the present set of measurements). The Yb moment at 1.5 K is quite small, $\mu_{Yb} = 0.57(9)\ \mu_B$, compared to the free ion value of about 4.54 μ_B for Yb^{3+}. This small value for the moment of Yb probably results from competition between the Kondo and RKKY interactions as described by Doniach [14].

4. Conclusions

$YbMn_2Si_2$ has been shown to exhibit collinear antiferromagnetic order, AF*il*, over the temperature range $T_{N1} \sim 526$ K $< T < T_{N2} \sim 30$ K. This behaviour is in common with most of the RMn_2X_2 rare earth intermetallic compounds (X = Si, Ge) for which $d_{Mn-Mn} \leqslant$ ∼2.85 A [9–11]. Below $T_{N2} \sim 30(5)$ K, the Mn magnetic sublattice $YbMn_2Si_2$ is found to exhibit a rearrangement to a more complicated antiferromagnetic structure in which re-ordering of the Mn moments takes place in the sequence +−−+ along the *c* axis with a doubling of the unit cell length associated with a propagation vector $\boldsymbol{k} = 00\frac{1}{2}$. The values of μ_{Mn} are found to remain essentially unchanged throughout this rearrangement of the antiferromagnetic ordering of the Mn lattice at the transition temperature $T_{N2} \sim 30(5)$ K. This novel low-temperature antiferromagnetic arrangement is maintained down to 1.5 K (the lowest temperature attained in the present work) at which temperature antiferromagnetic ordering of the Yb^{3+} ions is observed. Ordering of the Yb sublattice also occurs in a +−−+ sequence, while fitting in with a propagation vector $\boldsymbol{k} = 00\frac{1}{2}$. The ground state magnetic behaviour of $YbMn_2Si_2$, represented here for the first time, is shown by figure 2(c). The magnetic moment values for $YbMn_2Si_2$ at 1.5 K are $\mu_{Mn} = 1.98(7)\ \mu_B$ and $\mu_{Yb} = 0.57(9)\ \mu_B$. The low value for the Yb^{3+} ion compared with the free ion value of about 4.5 μ_B is probably due to the competition between the Kondo and RKKY interactions.

Acknowledgments

This work is supported in part by grants from the Australian Institute of Nuclear Science and Engineering. SJC acknowledges support from the Access to Major Research Facilities Program, Australian Nuclear Science and Technology Organisation.

References

[1] Nowik I, Felner I and Bauminger E R 1997 *Phys. Rev.* **55** 3033
[2] Levin E M, Palewski T and Kuzhel B S 1999 *Physica* B **259–261** 142
[3] Hofmann M, Campbell S J and Szytula A 2000 *J. Alloys Compd.* **311** 137
[4] Szytula A and Szott S 1981 *Solid State Commun.* **40** 199
[5] Nowik I, Felner I and Bauminger E R 1998 *J. Magn. Magn. Mater.* **185** 91
[6] Rodriguez-Carvajal J 1998 *FullProf 98, LLB*
[7] International Tables for Crystallography 1992 ed T Hahn vol C (Dordrecht, Holland: Reidel)
[8] Siek S, Szytula A and Leciejewicz J 1981 *Solid State Commun.* **39** 863
[9] Venturini G, Welter R, Ressouche E and Malaman B 1995 *J. Magn. Magn. Mater.* **150** 197
[10] Szytula A and Leciejewicz J 1994 *Handbook of Crystal Structures and Magnetic Properties of Rare Earth Intermetallics* (Boca Raton: CRC Press)
[11] Venturini G 1996 *J. Alloys Compd.* **232** 133
[12] Hagdorn K, Hohlwein D, Ihringer J, Knorr K, Prandl W, Ritter H, Schmid H and Zeiske Th 1999 *Eur. Phys. J.* B **11** 243
[13] Venturini G, Malaman B and Ressouche E 1996 *J. Alloys Compd.* **240** 139
[14] Doniach S 1977 *Physica* B **91** 231